

Electrochemical Growth of Polypyrrole Microcontainers

Liangti Qu, Gaoquan Shi,* Feng'en Chen, and Jiaxin Zhang

Department of Chemistry, Tsinghua University, Beijing 100084, P. R. China

Received July 23, 2002; Revised Manuscript Received November 18, 2002

ABSTRACT: Polypyrrole microcontainers with morphology like bowls, cups, and bottles have been electrochemically generated by direct oxidation of pyrrole in the aqueous solution of β -naphthalenesulfonic acid (β -NSA). The well-ordered microcontainers stand upright on the working electrode surface in a density of 2000–8000 units cm^{-2} . Their morphological features can be simply controlled by electrochemical polymerization condition, and the results have a good reproducibility. The growth process of microcontainers was studied by scanning electron microscopy. A “soup bubble” growth mechanism was postulated and confirmed by electrolysis of water using a polypyrrole film-coated electrode. The walls of the microcontainers were made of polypyrrole in the oxidized (conductive) state according to the results of Raman and infrared spectroscopies. Electrochemical studies demonstrated that the PPy film with microcontainers had a large surface area which resulted in high film/electrolyte double-layer capacitive charges.

Introduction

Micro- and nanostructured conducting polymeric materials have attracted increasing attention, mainly due to their potential applications in catalysis, optics, drug delivery, and microelectronics.^{1–3} Miniaturized systems (microreactors) for performing unit operations and reactions in chemical technology are also applied widely for process development.⁴ In addition, microcontainers and microchannels are important devices for microanalysis and microscale chemical and biochemical reactions. Furthermore, polypyrrole, due to its good biocompatibility with nervous tissue, can be applied to nerve regeneration.⁵ Therefore, polypyrrole microcontainers are expected to have important applications in microscale chemical or electrochemical reaction, single cell study, and cell clinics. Here, we describe the spectacular growth of polypyrrole microstructures with unusual morphologies like bowls, cups, and bottles by direct electrochemical oxidation of pyrrole in the aqueous solution of β -naphthalenesulfonic acid (β -NSA).

Experimental Section

Chemically pure β -NSA (Beijing Tongxian Yucai Fine Chemical Factory) was used as received, and pyrrole (Chinese Army Medical Institute) was distilled before use. The growth of polypyrrole (PPy) microstructures was carried out at room temperature in a one-compartment cell by the use of a model 283 potentiostat–galvanostat (EG&G Princeton Applied Research) under computer control. The working and counter electrodes were two stainless steel sheets (AISI 321) with surface area of 0.5 cm^2 each and placed 0.5 cm apart. All potentials were referred to a saturated calomel electrode (SCE). The solutions were deaerated by a dry nitrogen stream and maintained at a light overpressure during the experiments. The typical electrolyte was an aqueous solution of 0.53 mol L^{-1} pyrrole and 0.57 mol L^{-1} β -NSA.

The infrared spectra were obtained by the use of a Spectrum GX FT-infrared spectrometer of Perkin-Elmer Co. Raman spectra were recorded by using a RM 2000 microscopic confocal Raman spectrometer (Renishaw PLC, England) employing a 633 nm laser beam at 0.1 mW and a CCD detector with 4 cm^{-1} resolution. The spectrum was accumulated three times for 30

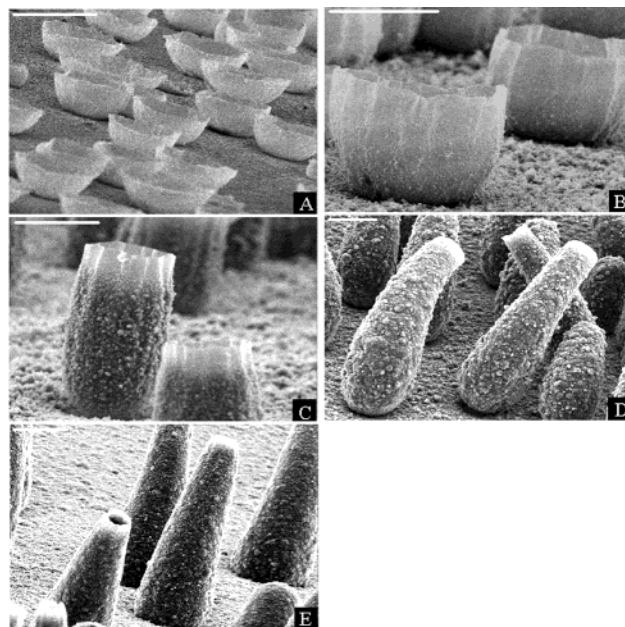


Figure 1. SEM images of the polypyrrole microstructures formed by electrolysis of pyrrole for 120 s at constant potentials of 0.8 V (A), 1.0 V (B), and 1.2 V (C, D, E). The typical electrolyte was the aqueous solution of 0.53 mol L^{-1} pyrrole and 0.57 mol L^{-1} β -NSA. The gourdlike (D) and bottlelike (E) microstructures were generated in the media containing 0.28 and 0.15 mol L^{-1} β -NSA, respectively. Scale bars: 100 μm .

s each. The morphology of the microstructures was studied using a KYKY2800 scanning electron microscope (Beijing Scientific Instrument Co.) after sputter-coating the microstructures with gold. Dynamic light scattering tests were carried out on a DLS-700 dynamic light scattering spectrophotometer (Stsuka) at room temperature. The specific surface areas of the microstructures were determined by the nitrogen absorption BET method (ASAP2010, Micromeritics).

Results and Discussion

Morphology. Figure 1 shows the scanning electron micrographs (SEMs) of the polypyrrole microcontainers prepared potentiostatically in the aqueous solution of 0.53 mol L^{-1} pyrrole and 0.57 mol L^{-1} (A–C) or 0.28

* Corresponding author: e-mail gshi@tsinghua.edu.cn; Fax 86-10-62771149.

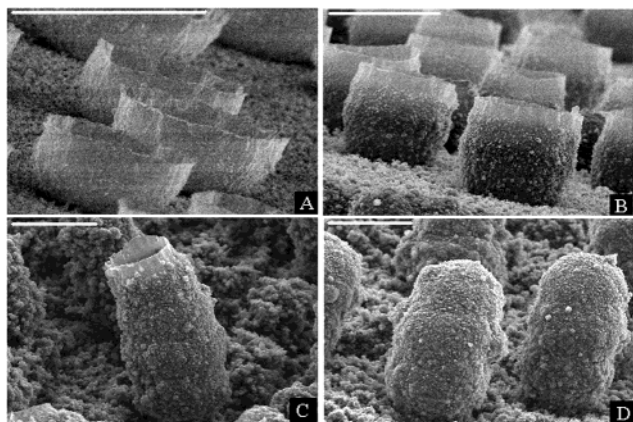


Figure 2. SEM images of the microstructures obtained by cyclic voltammetric scanning in the potential scale of 0–1.2 V for different cycles (A, 1; B, 3; C, 5; D, 6). Potential scan rate: 20 mV s^{-1} . Scale bars: 100 μm .

mol L^{-1} (D) or 0.15 mol L^{-1} (E) β -NSA. It is clear from this figure that the microcontainers stand upright on the electrode surface. They have fairly good uniformity and align in a high density of 2000–8000 units cm^{-2} . The microbowls (Figure 1A,B) and microcups (Figure 1C) were formed by electrolysis at constant potentials of 0.8, 1.0, and 1.2 V for 120 s each, respectively. The wall of the microbowls (Figure 1A,B) is semitransparent, and its outside and inner side surfaces are smooth. With the increase of applied potential from 0.8 to 1.0 V, the height of the bowls increased from ca. 45 to ca. 100 μm , and their caliber also increased from ca. 100 to 120–150 μm . When a constant potential of 1.2 V was applied, the “bowls” turned into “cups”, and their height was increased to over 200 μm . It is obvious that the height of the microstructures can be controlled by changing the value of the applied potential. The morphology of the microstructures also depends on the concentration of β -NSA. As β -NSA concentration changed from 0.57 mol L^{-1} to 0.28 mol L^{-1} or to 0.15 mol L^{-1} , the morphology of the microstructures grown at 1.2 V for 120 s changed into microgourds (Figure 1D) or microbottles (Figure 1E) with the height of about 400 μm , respectively. The caliber of the gourds is around 70 μm , and that of the bottles is about 50 μm . These indicated that the decrease of β -NSA concentration was in favor of the formation of polypyrrole microtubules and led the caliber of the microcontainers to decrease.

The microstructures obtained by cyclic voltammetric scanning in the potential scale of 0–1.2 V for different cycles are shown in Figure 2. Although they have different shapes, the diameter of the microcontainers is almost the same and close to 100 μm . With the increase of cycling number from 1 to 5, the microbowls (Figure 2A) turn into microcups (Figure 2B,C) and the height of the microstructures also increases from ca. 50 μm (Figure 2A) to ca. 220 μm (Figure 2C). However, the ratio of caliber and diameter of the body decreases with the increase of cycling number. As the CV was carried out for six cycles, the mouths of the microcups were sealed and hollow bodies (Figure 2D) were formed. This implies that the microcontainers can be applied for encapsulation of micron-sized materials.

Figure 3 shows the SEM images of the microstructures grown by voltammetric scanning for three cycles in the range of 0 V to different switching potentials. It is clear from Figure 3A–E that the caliber and height of the microcups increase gradually with the increase

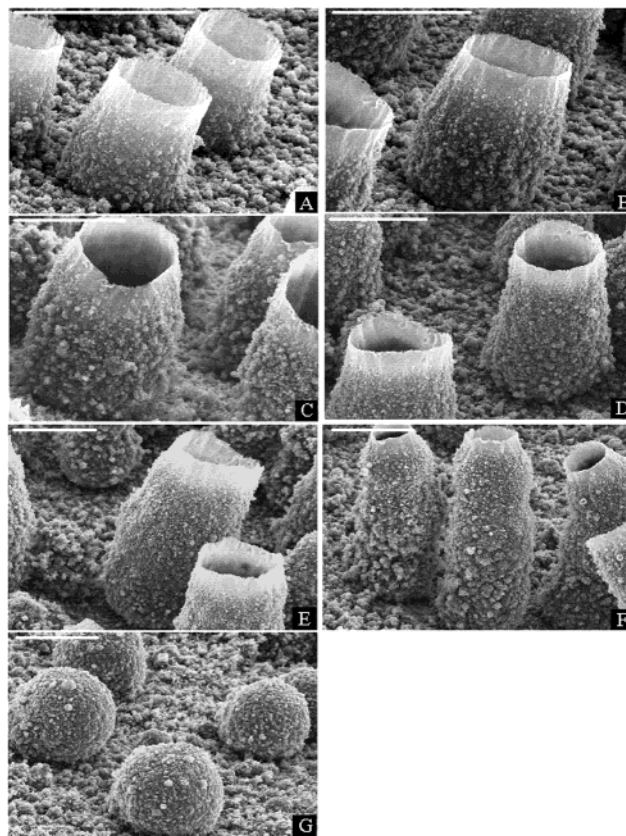


Figure 3. SEM images of the microstructures obtained by cyclic voltammetric scanning for three cycles in different potential scales (A, 0–0.9 V; B, 0–1.0 V; C, 0–1.1 V; D, 0–1.2 V; E, 0–1.3 V; F, 0–1.4 V; G, 0–1.6 V). Potential scan rate: 20 mV s^{-1} . Scale bars: 100 μm .

of switching potential. The caliber and height of the microcups shown in Figure 3A are about 50 μm and 60 μm , respectively. However, those in Figure 3E are found to be about 100 μm and 200 μm . In the potential scale of 0–1.4 V, the height of the microcups increases to about 230 μm , while the caliber of the microcups decreases to around 65 μm (Figure 3F). When the switching anodic potential changed to 1.6 V, no microcups formed, and only spheres with a diameter of about 110 μm were observed (Figure 3G). This indicates that a high switching potential supports the closure of the microstructures.

The potential scan rate of CV also has a strong effect on the morphology of the microstructures. Figure 4 illustrates the SEM images of the microstructures produced by voltammetric cycle in the potential scale of 0–1.2 V for four cycles at different potential scan rate. At the potential scan rate of 20 mV s^{-1} , the microcups with caliber of about 100 μm and height of about 200 μm were formed (Figure 4A). When the potential scanning rate was increased to 50 mV s^{-1} , the size of the microcups decreased; their caliber and height are only 40 μm and 80 μm , respectively. At the potential scan rate of 100 mV s^{-1} , only hollow spheres with a diameter of about 30 μm were generated on the surface of the electrode.

By modulating the electrochemical condition, the microcontainers with different height, caliber, and shape can be obtained. As a result, the morphology of the polypyrrole microstructures can be controlled simply by changing the electrolysis conditions. A typical example is the potential control growth of the “goblet” (Figure

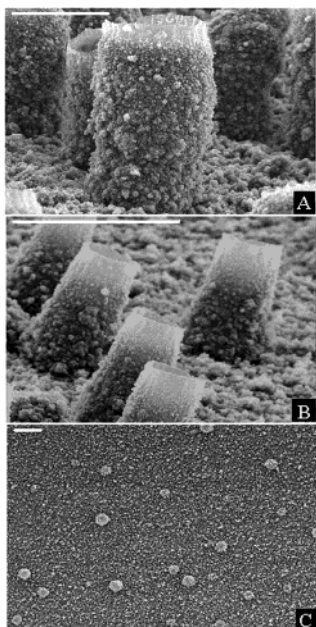


Figure 4. SEM images of the microstructures produced by potential cycling in the scale of 0–1.2 V for four cycles at different potential scan rate (A, 20 mV s^{-1} ; B, 50 mV s^{-1} ; C, 100 mV s^{-1}). Scale bars: 100 μm .

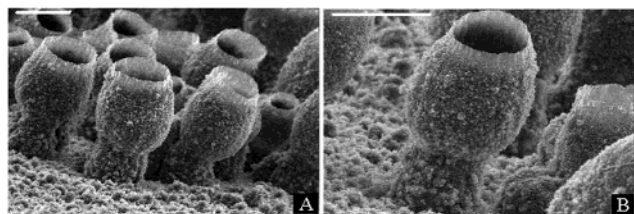


Figure 5. SEM image of the gobletlike microstructures formed by electrolysis at a constant potential of 1.2 V for 40 s and successively 0.75 V for 120 s and then 1.4 V for 60 s. Scale bars: 100 μm .

5). The “goblets” have thin root parts (80–90 μm , grown at 1.4 V for 40 s), a wide middle part (120–130 μm , grown at 0.75 V for 120 s), and small mouths (80–90 μm , grown at 1.4 V for 60 s).

PPy microstructures also can be generated in other systems with different metallic electrodes or surfactants. Figure 6 demonstrates the cuplike microstructures formed by electrolysis of 0.53 mol L^{-1} pyrrole in 0.57 mol L^{-1} β -NSA aqueous solution at 1.4 V for 120 s on a gold-coated SS electrode (A) and Pt (B) electrode. They have features similar to the microstructures grown on an SS electrode. Electrolysis of pyrrole in a (+)- or (–)-camphorsulfonic acid aqueous solution can grow the aligned microcontainers, too (C, D). (The details will be reported elsewhere.) However, the microstructures generated in the medium of aqueous sodium dodecylbenzenesulfonate (SDBS) were quite different. They have morphology like plates (E, F). This may be due to that the PPy films grown in a basic medium have a lower doping level and weaker strength than those grown in an acidic medium.

Infrared and Raman Measurements. The microscopic Raman spectra (the laser spots focused on the wall, bottom, inside, and outside surfaces give the spectra with similar features) and transmission infrared spectra (with KBr pellets) of the microstructures indicated the microstructures were made of polypyrrole films in the doped (conductive) state.^{6–11} Figure 7 shows

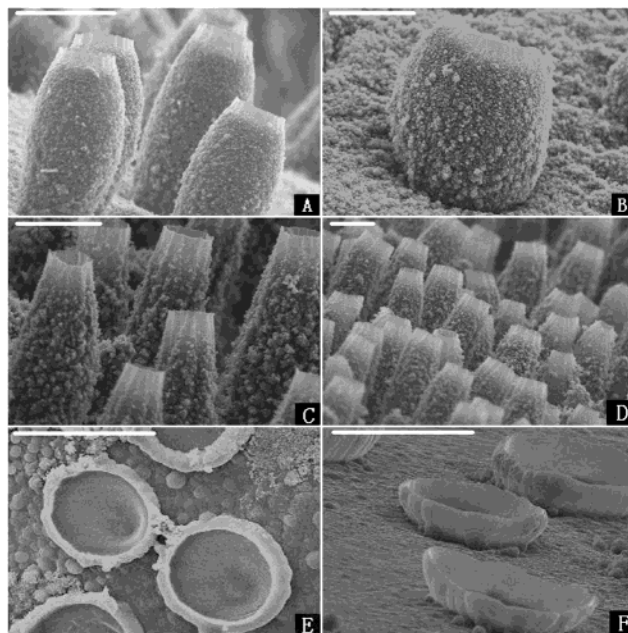


Figure 6. SEM images of PPy microstructures generated in different systems. (A) and (B) were formed by electrolysis of 0.53 mol L^{-1} pyrrole in 0.57 mol L^{-1} aqueous β -NSA solution at 1.4 V for 120 s on a gold-coated stainless steel electrode and a Pt electrode, respectively. (C) and (D) were obtained by electrolysis of 0.5 mol L^{-1} pyrrole at 1.0 V for 240 s in 0.6 mol L^{-1} aqueous (+)- and (–)-CSA aqueous solutions, respectively. The platelike microstructures (E, F) were generated by electrolysis of 0.26 mol L^{-1} pyrrole in 0.28 mol L^{-1} aqueous SDBS solution at 1.6 and 1.4 V for 240 s each, respectively. Scale bars: 100 μm .

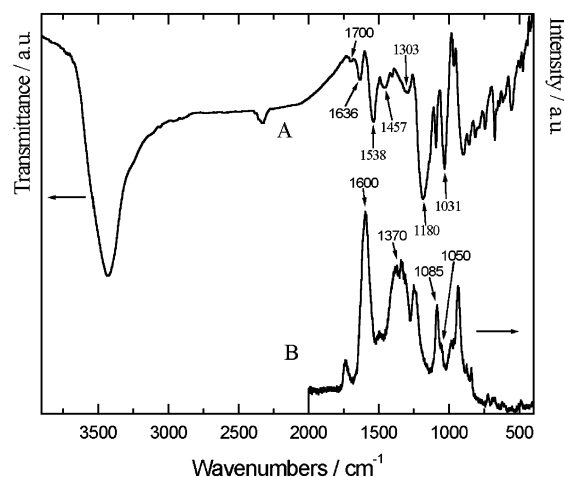


Figure 7. Transmission infrared spectrum (with KBr pellets) (A) and microscopic Raman spectrum (B) of a PPy film with microcups.

the typical Raman and infrared spectra of the microcups prepared in the aqueous solution of β -NSA. The infrared bands at 1636 and 1031 cm^{-1} (Figure 7A) are attributed to the naphthalene ring and $-\text{SO}_3^-$ group of the dopants, respectively. This indicates the PPy is doped by β -NSA. The 1538 cm^{-1} band is assigned to the stretching vibration of the C–C double bond and the C–C single bond of PPy–NSA. The C–N stretching vibration bands of PPy appear at 1457 and 1180 cm^{-1} .^{6–8} Furthermore, the weak absorption band in the region around 1700 cm^{-1} is attributed to the carbonyl group, which indicates that the polymer was only slightly overoxidized during the growth process.⁹ The Raman band at ca. 1600 cm^{-1} represents the backbone

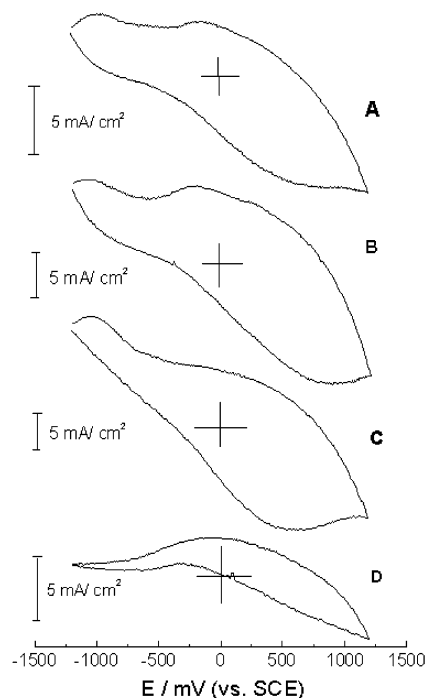


Figure 8. Cyclic voltammograms of the polypyrrole film with microcups (A; 8.6 C cm^{-2}), microbowls (B; 2.9 C cm^{-2}), microgourds (C; 5.7 C cm^{-2}), and a flat polypyrrole film (D; 10.0 C cm^{-2}) in MeCN containing 0.1 mol L^{-1} tetrabutylammonium tetrafluoroborate (TBATFB) at a potential scan rate of 100 mV s^{-1} . The flat polypyrrole film was prepared at potential 1.2 V in the aqueous solution of $0.1 \text{ mol L}^{-1} \text{ LiClO}_4$ and 0.53 mol L^{-1} pyrrole.

stretching mode of $\text{C}=\text{C}$ bonds (Figure 7B). The strong bands at ca. 1370 and 1085 cm^{-1} belong to the ring stretching and the $\text{N}-\text{H}$ in-plane deformation of the oxidized (doped) species, respectively.^{10,11} The corresponding band of neutral species at 1050 cm^{-1} is relatively weak.

Electrochemical Properties. The cyclic voltammograms of the PPy film with microcups (Figure 8A), microbowls (Figure 8B), or microgourds (Figure 8C) showed a couple of strong and broad oxidation and reduction waves. Their wave currents were much stronger than those of the flat film deposited on the same electrode (Figure 8D). This is mainly due to the fact that the surface area of the polypyrrole film with microstructures is much larger than that of a normal film, which results in much higher film/electrolyte double-layer capacitive charges. The surface area of the PPy film with the cuplike microstructures grown for 5 C cm^{-2} is about 90 times that of the flat film grown for the same charge density as measured by N_2 absorption. Therefore, the PPy films with microstructures may have potential applications in fabrication of high-quality microelectronics such as capacitors and sensors.

Formation Mechanism. β -NSA is a typical surfactant and micelles can be formed in its aqueous solution. Dynamic light scattering tests showed that the micelles in the aqueous solution of 0.53 mol L^{-1} pyrrole and $0.57 \text{ mol L}^{-1} \beta$ -NSA had an average diameter of 354 nm . This value is far smaller than the size of the PPy microstructures ($\sim 100 \mu\text{m}$). Therefore, it is illogical to explain the formation of the microstructures by a micelles template mechanism. On the other hand, careful observation during the electrochemical synthesis can find that small gas bubbles release from the surface of working electrode. The microbubbles on the electrode surface also

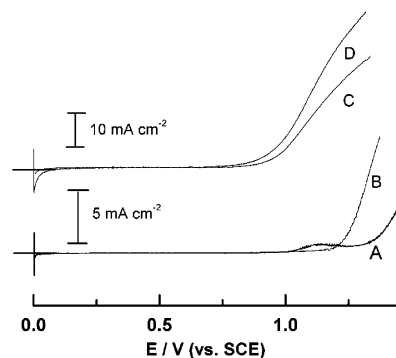


Figure 9. Anodic polarization curves of $0.57 \text{ mol L}^{-1} \beta$ -NSA aqueous electrolyte at pristine SS (A), Pt (B) electrode or a polypyrrole film with microstructure (1.0 C cm^{-2}) coated SS (C), Pt (D) electrode at a potential scan rate of 20 mV s^{-1} .

can be observed clearly with a microscope. An electrochemical study confirmed that the gas bubbles resulted from water decomposition. As shown in Figure 9, the polarization curve of a pristine stainless steel (SS) electrode in $0.57 \text{ mol L}^{-1} \beta$ -NSA aqueous solution showed a weak passivation wave of the electrode at ca. 1.0 V and a strong anodic current wall of water decomposition (Figure 9A). The onset oxidation potential of water is read to be 1.25 V (vs SCE), which is very close to the reported value (1.23 V vs SCE).¹² In comparison, the onset oxidation potential of the electrolyte at a polypyrrole film with microcups-coated SS electrode was found to be at only ca. 0.8 V (Figure 9C), which implied that the polypyrrole film could catalyze the decomposition of water. The oxidation wave of PPy and the passivation wave of the electrode are too weak to be observed clearly from this curve. To confirm the catalytic effect of polypyrrole film, a platinum (Pt) sheet was used as working electrode to replace the SS electrode. The decomposition potential of $0.57 \text{ mol L}^{-1} \beta$ -NSA aqueous solution at pristine Pt electrode is at ca. 1.23 V (Figure 9B), in accordance with the reported value.¹² However, the oxidation potential of water at a polypyrrole film-coated Pt electrode was also found at only ca. 0.8 V (Figure 9D), which is in good agreement with that shown in Figure 9C. Li and Qian also reported that oxygen gas could be generated by electrolysis of acidic water ($\text{pH} = 3$) on a PPy-coated Pt electrode in a fairly low potential region ($0.8\text{--}1.1 \text{ V}$ vs SCE).⁹ On the other hand, cyclic voltammetric studies demonstrated that the oxidation wave of polypyrrole film in a $0.57 \text{ mol L}^{-1} \beta$ -NSA aqueous solution was at ca. 0.5 V . This result confirms the oxidation waves (at ca. 0.8 V) in Figure 9C,D are not caused by the oxidation of polypyrrole. Accordingly, it is reasonable to conclude that the bubbles were produced by the decomposition of water. The gas bubbles and the aqueous solution containing the monomer and β -NSA or SDBS (they are typical surfactants) lead to the formation of "soap bubbles". The growth of polypyrrole around these bubbles results in the microstructures described above. Therefore, the formation of the unusual microstructures can be attributed to the function of "soap bubble" or "gas bubble" templates analogous to a scheme reported previously.¹³ The "soap bubble" size and generation rate and the growth rate of polypyrrole film depend strongly on the experimental conditions. Thus, changing the electrolysis conditions can modulate the shape, size, and caliber of the polypyrrole microstructures. No microstructures were generated at the potentials lower than 0.8 V , and the microstructures were grown on PPy films (do not come

in contact with the metallic electrode directly). These observations also supported the mechanism described above.

Conclusions

Polypyrrole microcontainers with very unusual morphology can be generated by electropolymerization of pyrrole in an aqueous solution of β -NSA. The shape and size of the microstructures can be modulated electrochemically. The walls of the microstructures are made of PPy in the doped state. The PPy films with microstructures showed strong and broad redox waves in the electrolyte of MeCN containing TBATFB because of their large surface areas. The microcontainers have many potential applications including picoscale chemistry, and the technology developed by this study can be extended to synthesize other materials with similar microstructures by changing monomers and surfactants.

Acknowledgment. This work is supported by National Natural Science Foundation of China.

References and Notes

- (1) Pool, R. *Science* **1990**, *247*, 1410.
- (2) Wan, M.; Huang, J.; Shen, Y. *Synth. Met.* **1999**, *101*, 708.
- (3) Martin, C. R. *Science* **1994**, *266*, 1961.
- (4) Ehrfeld, W.; Hessel, V.; Haverkamp, V. *Microreactors. Ullmann's Encyclopedia of Industrial Chemistry*; Wiley-VCH: Weinheim, 1999.
- (5) Chen, S. J.; Wang, K. Y.; Yuan, C. W.; et al. *J. Mater. Sci., Lett.* **2000**, *19*, 2157.
- (6) Mathy, G. I.; Truong, V. T. *Synth. Met.* **1997**, *89*, 103.
- (7) Lei, J.; Liang, W.; Martin, C. R. *Synth. Met.* **1992**, *48*, 301.
- (8) Tian, B.; Zerbi, G. *J. Chem. Phys.* **1990**, *92*, 3886.
- (9) Li, Y. F.; Qian, R. Y. *Electrochim. Acta* **2000**, *45*, 1727.
- (10) Liu, Y. C.; Hwang, B. J.; Jian, W. J.; Santhanam, R. *Thin Solid Films* **2000**, *374*, 85.
- (11) Mikat, J.; Orgzall, I.; Hochheimer, H. D. *Phys. Rev. B* **2002**, *65*, 174202.
- (12) Sakmeche, N.; Aeiya, S.; Aaron, J. J.; Jouini, M.; Lacroix, J. C.; Lacaze, P. C. *Langmuir* **1999**, *15*, 2566.
- (13) Sutton, S. J.; Vaughan, A. S. *Polymer* **1996**, *37*, 5367.

MA021177B